Electronic Supplementary Material (ESI) for New Journal of Chemistry.

Electronic Supplementary Information (ESI) for

Luminescent Sensing, Electrochemical, and Magenetic Properties of 2D Coordination Polymers Based on the Mixed Ligands of *p*-Terphenyl-2,2'',5'',5'''-tetracarboxylate Acid and 1,10-phenanthroline

Liming Fan,*[a,b] Zhangjie Liu,[a] Yujuan Zhang,[a] Feng Wang,[a] Dongsheng Zhao,[a] Jiandong Yang,[a] Xiutang Zhang*[a]

[a]*Department of Chemistry, College of Science, North University of China, Taiyuan 030051, China.*
b Shandong Provincial Key Laboratory of Chemical Energy Storage and Novel Cell Technology, School of Chemistry and Chemical Engineering, Liaocheng University, Liaocheng, 252059, China.

E-mail: limingfan@nuc.edu.cn; *xiutangzhang@163.com*.

Table of Contents

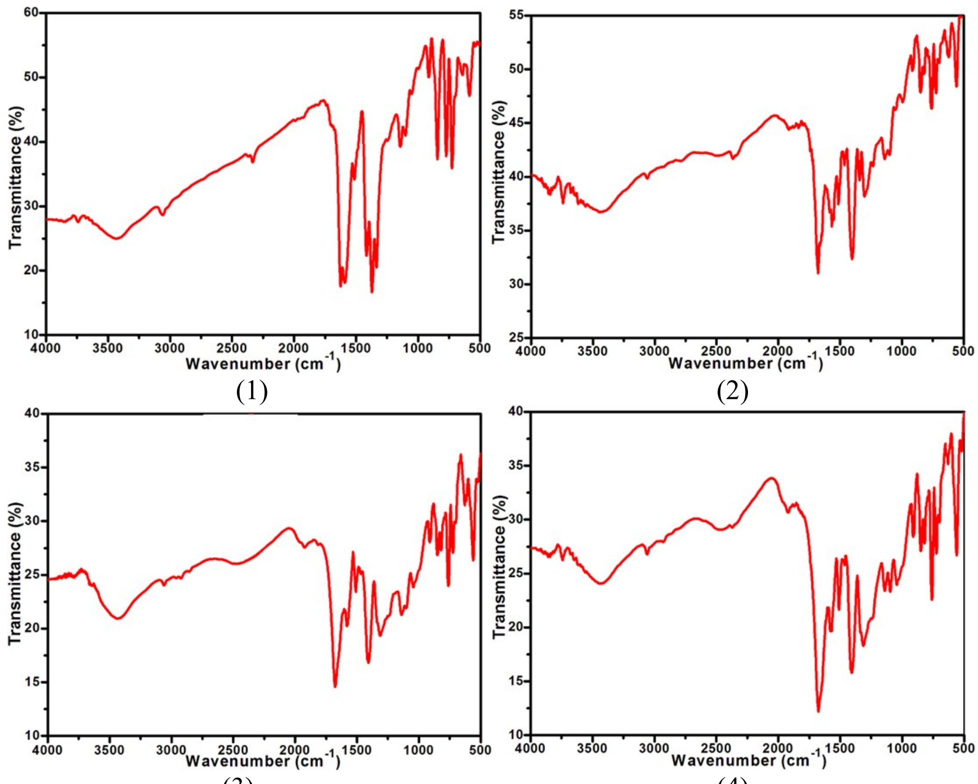

Fig. S1 The IR spectra of CPs **1-4**.

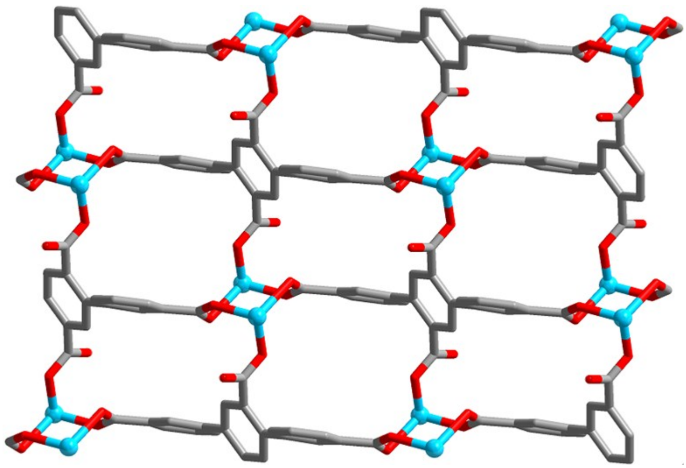

Fig. S2 The 2D $[Cu(tptc)_{0.5}]_n$ sheet in CP **1**.

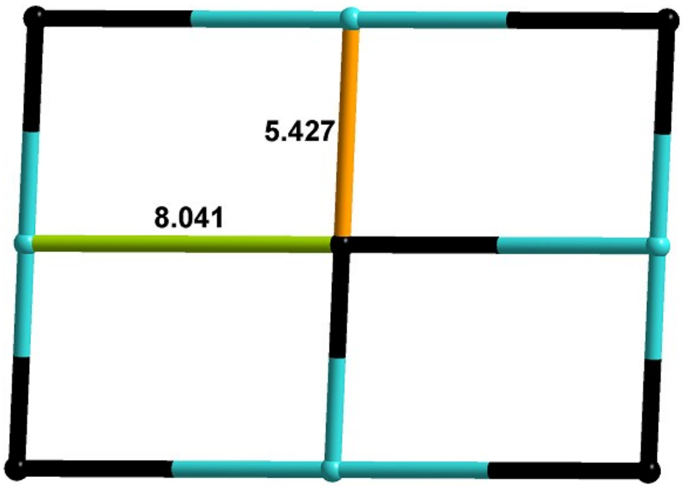

Fig. S3 The (4,4)-connected $\{4^4 \cdot 6^2\}$-**sql** sheet of CP **1**.

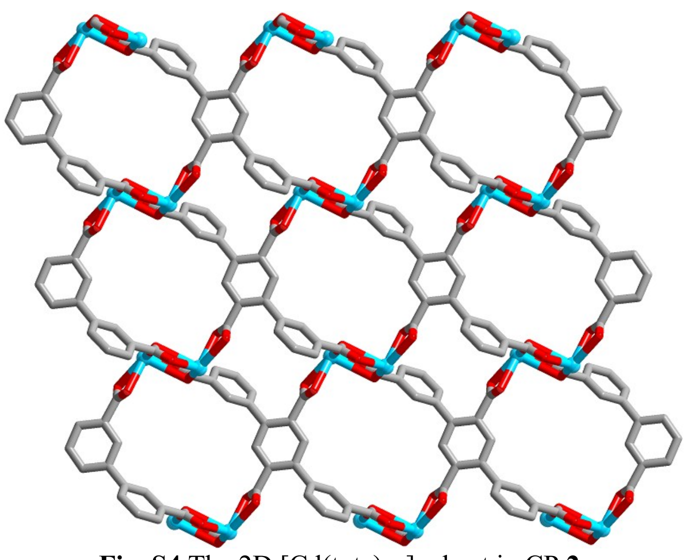

Fig. S4 The 2D $[Cd(tptc)_{0.5}]_n$ sheet in CP **2**.

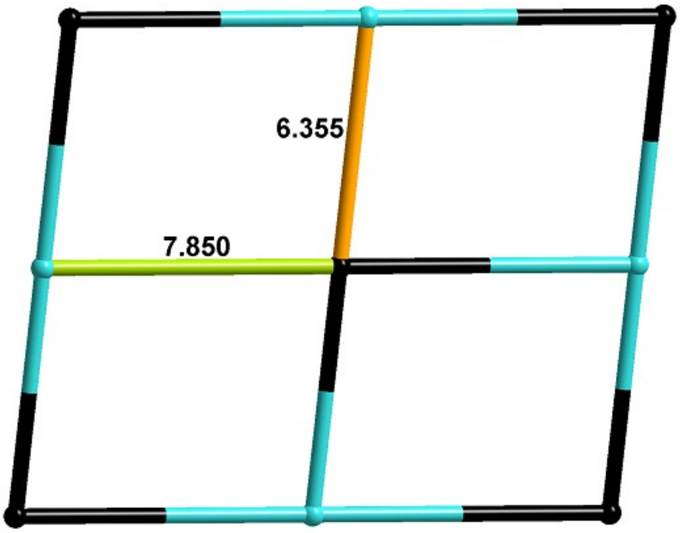

Fig. S5 The (4,4)-connected $\{4^4 \cdot 6^2\}$-**sql** sheet of CP **2**.

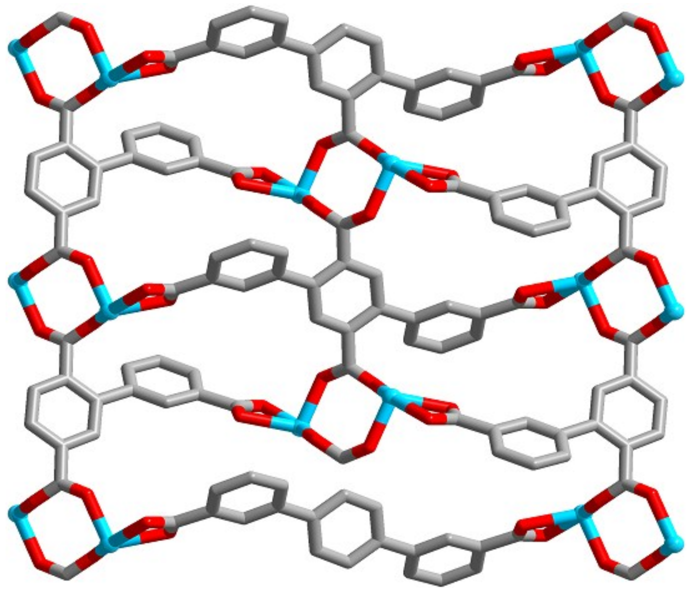

Fig. S6 The 2D $[Mn(tptc)_{0.5}]_n$ sheet in CP **3**.

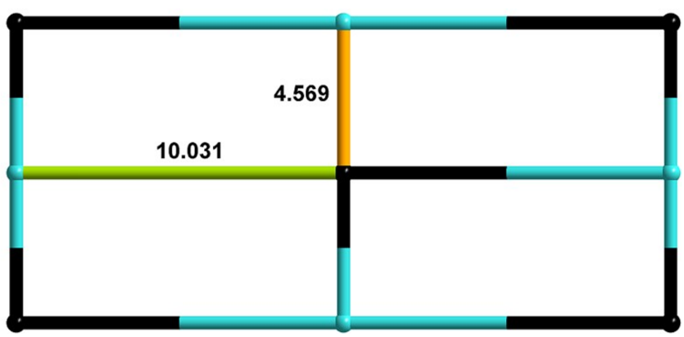

Fig. S7 The (4,4)-connected $\{4^4 \cdot 6^2\}$-**sql** sheet of CP **3**.

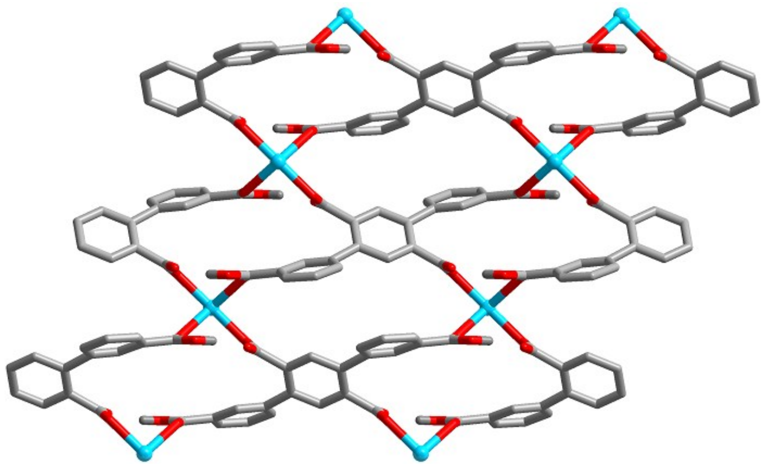

Fig. S8 The 2D $[Mn(H_2tptc)]_n$ sheet in CP **4**.

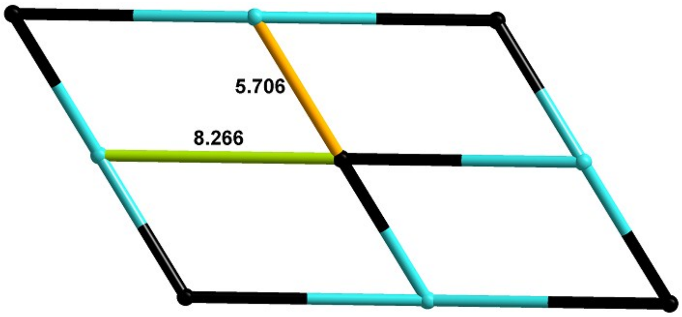

Fig. S9 The (4,4)-connected $\{4^4{\cdot}6^2\}$**-sql** sheet of CP **4**.

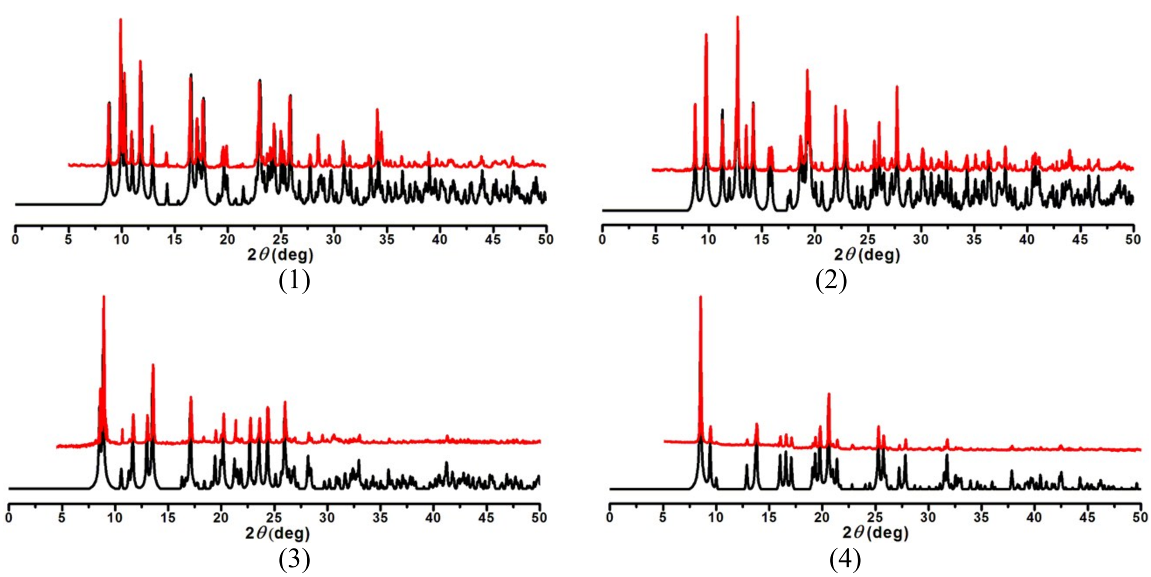

Fig S10. PXRD patterns of **1-4**. Dark: calculated from the X-ray single-crystal data; Red: observed for the as-synthesized solids.

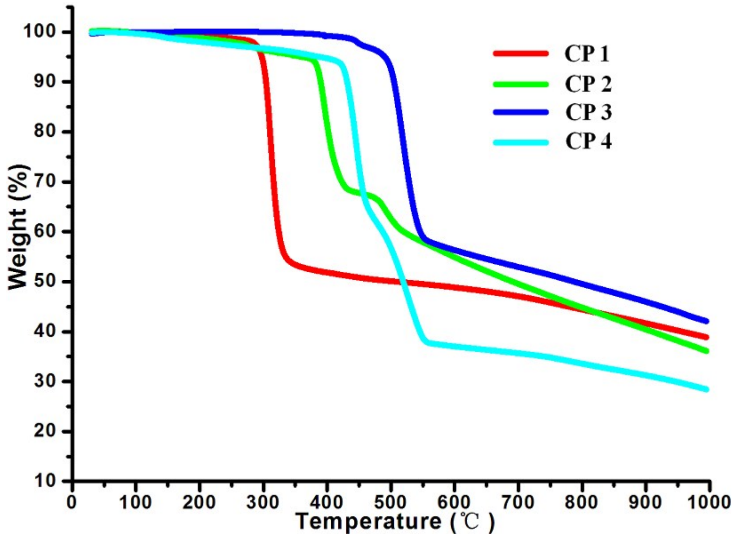

Fig S11. TGA curves for CPs **1−4**.

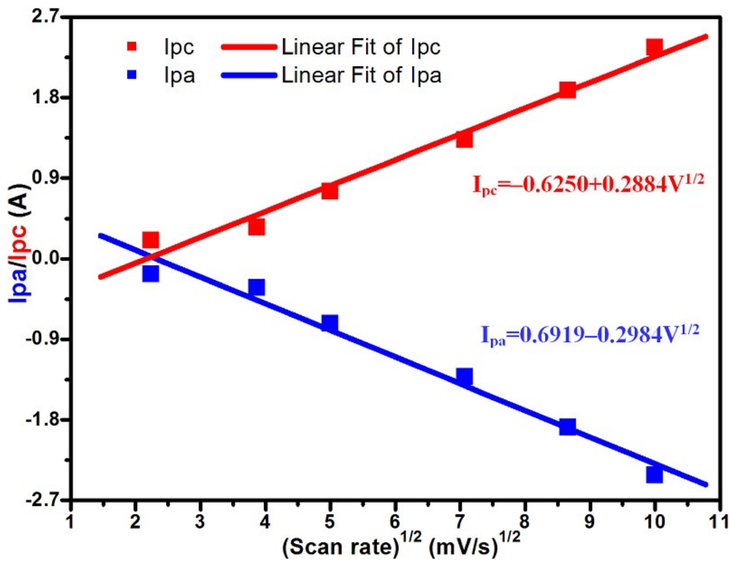

Fig S12. The voltammetric current as a function of square root of scan rate of CP **1** as electrode.

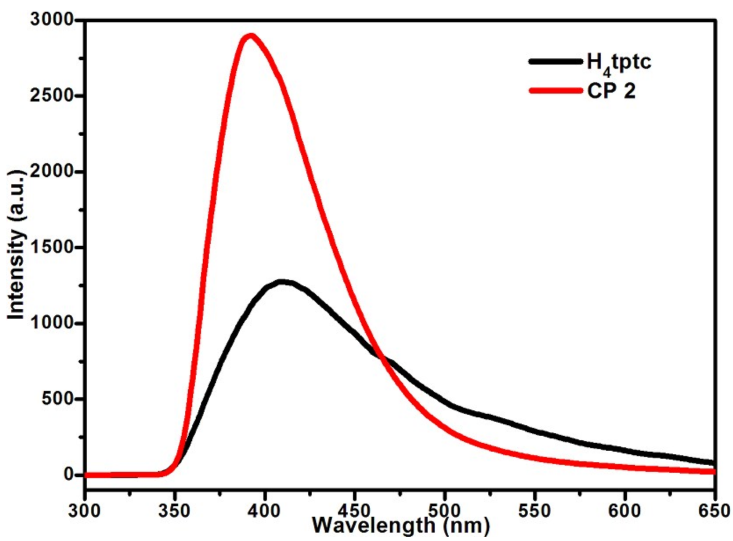

Fig S13. The fluorescence spectrum of free H_4tptc and CP **2** in solid state at room temperature.

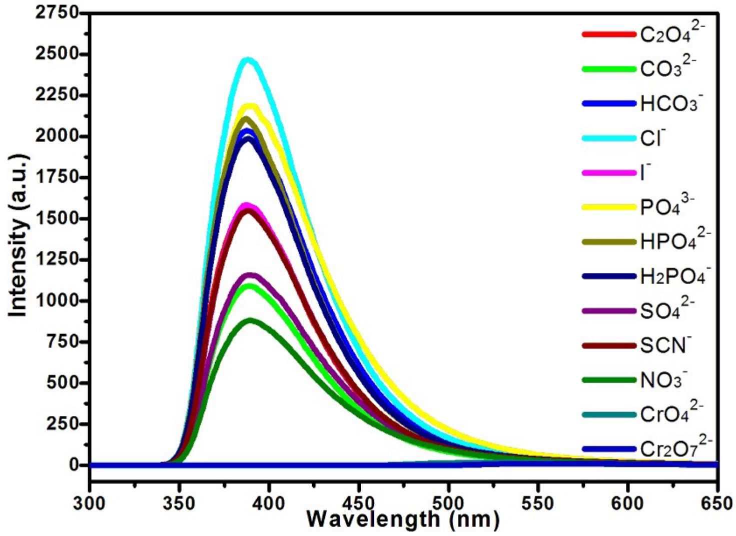

Fig S14. The luminescence intensities of CP **2** which were dispersed in the aqueous solution of different anions.

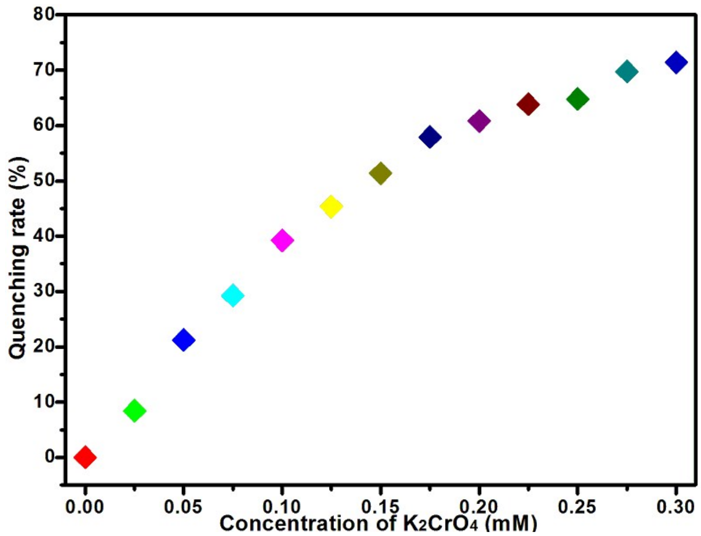

Fig S15. The quenching rate of CP **2** with different concentrations of K_2CrO_4 in aqueous solution.

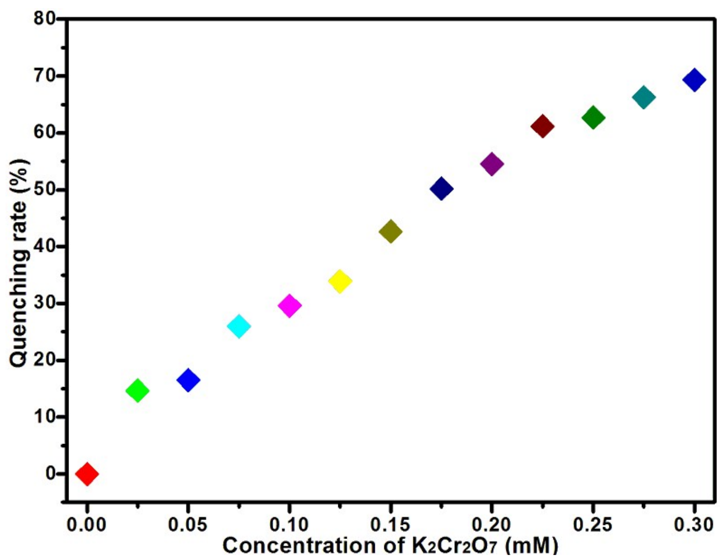

Fig S16. The quenching rate of CP **2** with different concentrations of $K_2Cr_2O_7$ in aqueous solution.

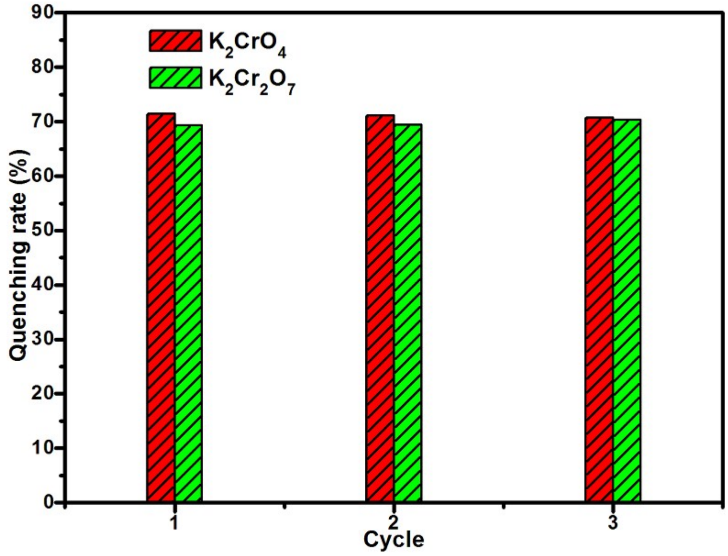

Fig. S17 The repeatability of Cr(VI) anions for CP **2** for three cycles.

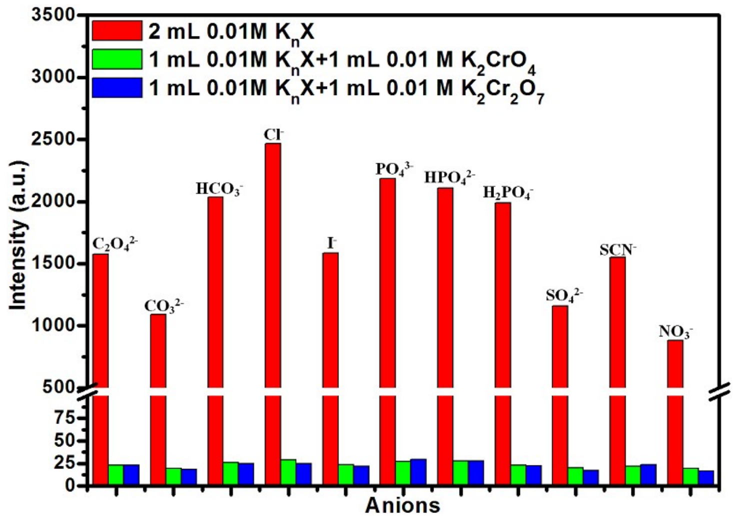

Fig. S18 The anti-interferences of CP **2** in sensing of $CrO_4^{2-}/Cr_2O_7^{2-}$ anions from normal anions in aqueous solution.

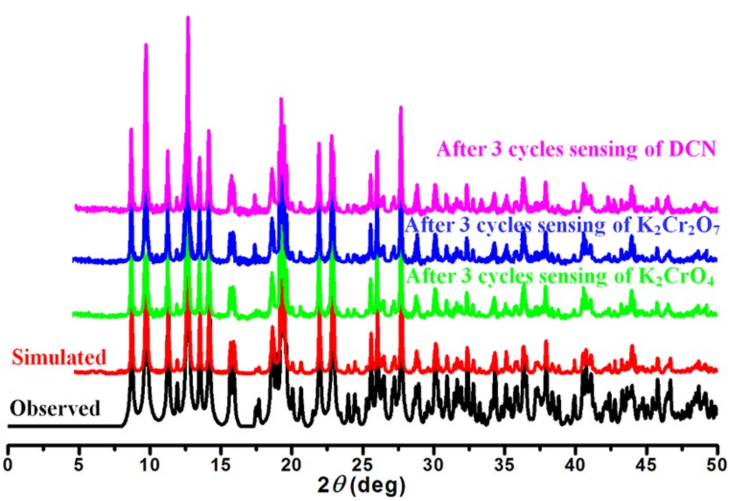

Fig S19. PXRD patterns of CP **2** after three cycles sensing of Cr(VI) anions in aqueous solution and DCN in DMF solution.

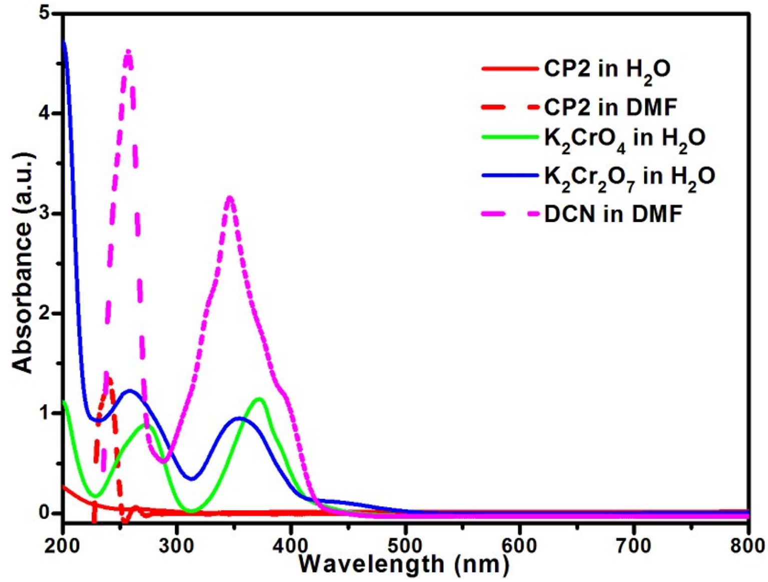

Fig S20. The UV-Vis absorbance spectrum of Cr(VI) anions in aqueous solution and DCN in DMF solution and the UV-Vis absorbance spectrum of CP **2**.

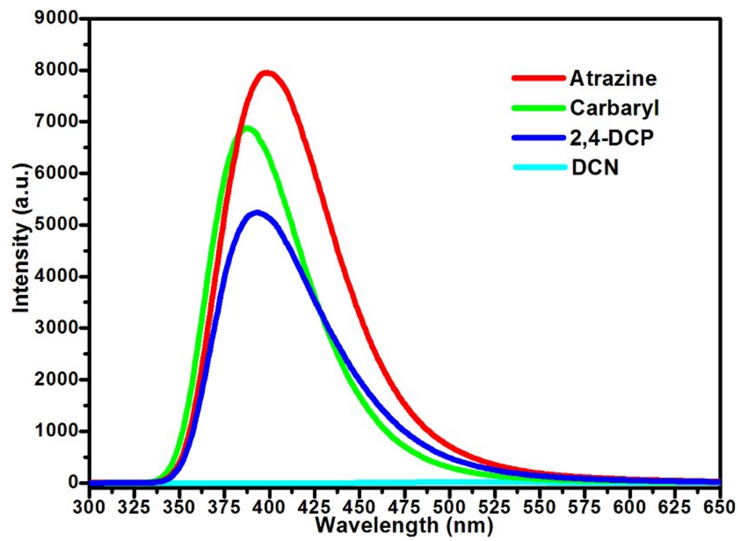

Fig S21. The luminescence intensities of CP **2** which were dispersed in the DMF solution of different pesticides.

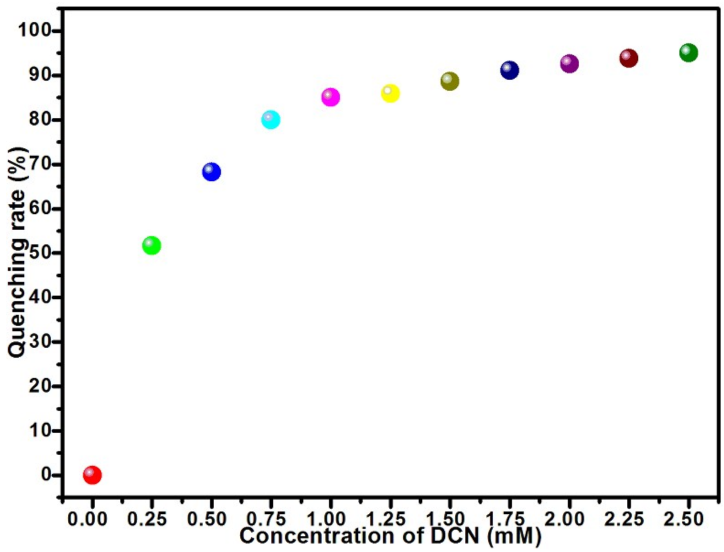

Fig S22. The quenching rates of CP **2** with different concentrations of DCN in DMF solution.

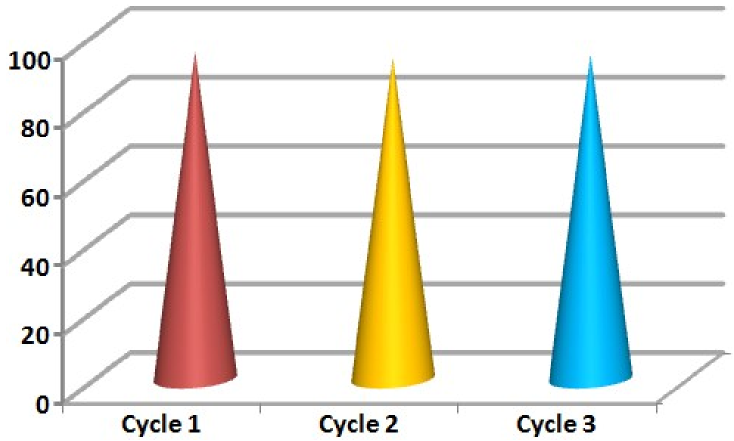

Fig. S23 The quenching rates of DCN for CP **2** for three cycles.

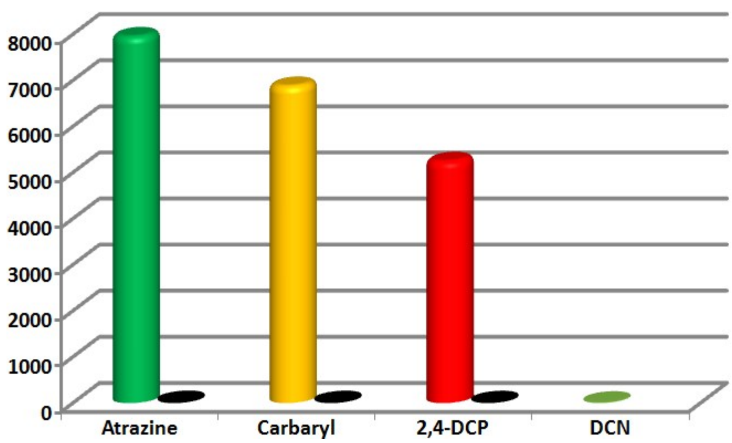

Fig. S24 The anti-interferences of CP **2** in sensing of DCN from normal pesticides in DMF solution.

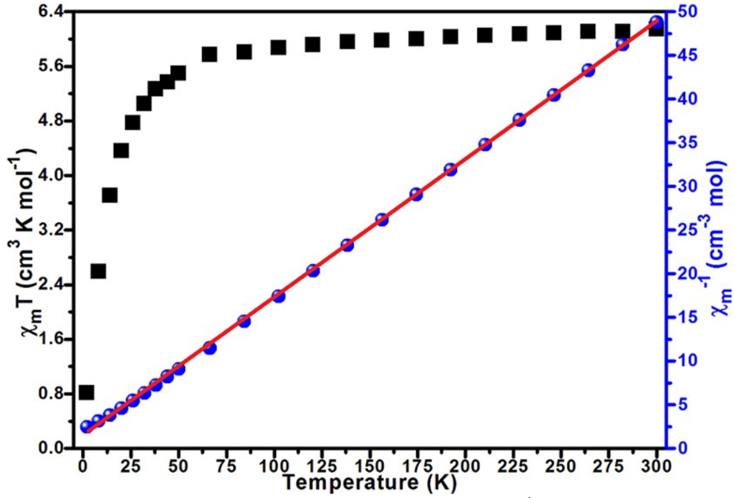

Fig S25. Temperature dependence of χ_mT and χ_m^{-1} for **3** under 1000 Oe.

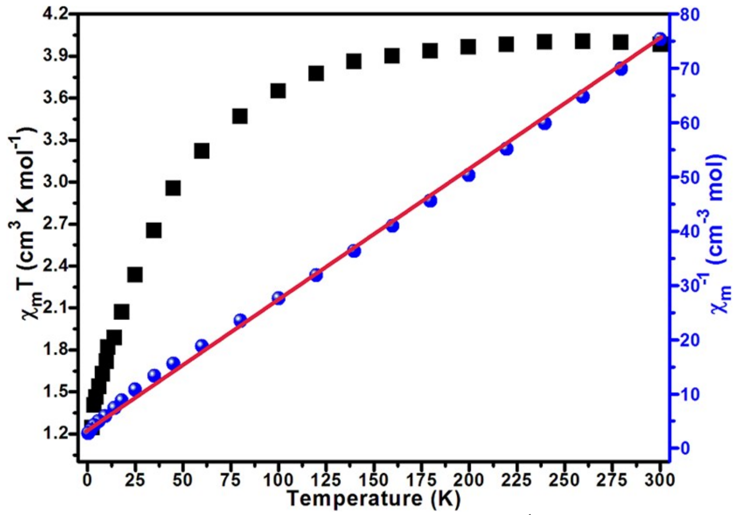

Fig S26. Temperature dependence of χ_mT and χ_m^{-1} for **4** under 1000 Oe.

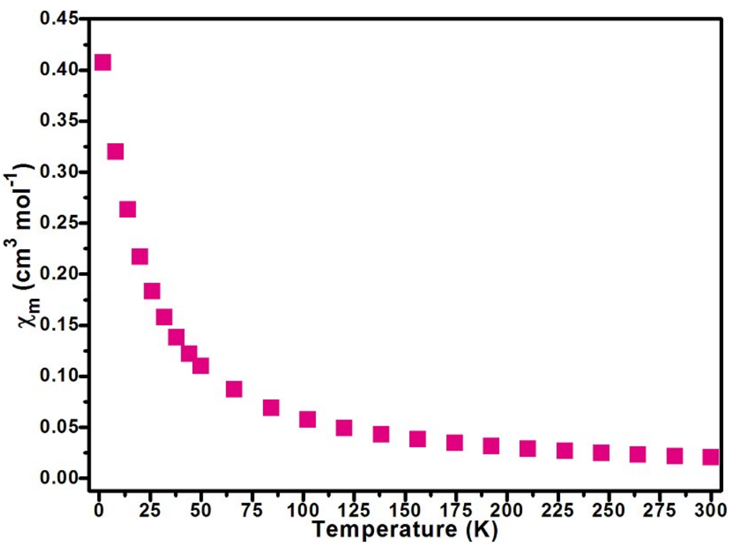

Fig S27. The χ_m *versus* T of CP **3**.

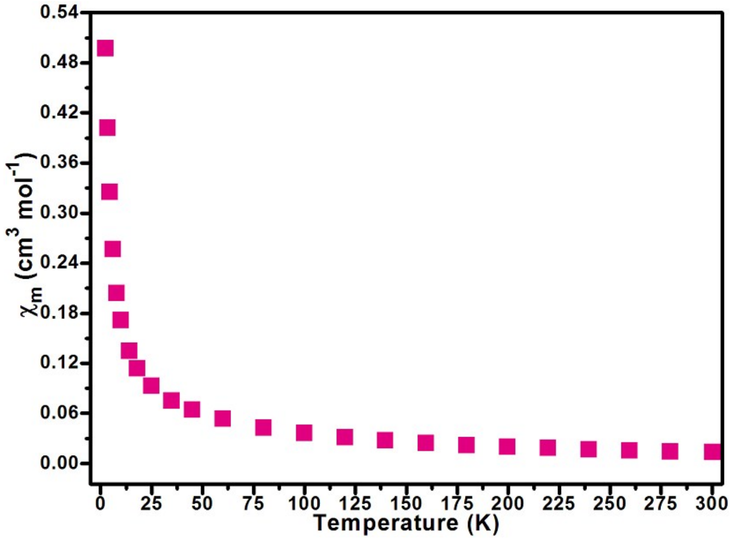

Fig S28. The χ_m *versus* T of CP **4**.

Table S1 Crystal data for **1–4**.

CP	**1**	**2**	**3**	**4**
Formula	$C_{23}H_{13}CuN_2O_4$	$C_{46}H_{26}Cd_2N_4O_8$	$C_{23}H_{13}MnN_2O_4$	$C_{34}H_{20}MnN_2O_8$
Formula weight	444.89	987.56	436.29	639.46
Crystal system	Triclinic	Triclinic	Monoclinic	Monoclinic
Space group	*P*-1	*P*-1	*C*2/c	*I*2/a
a (Å)	9.281(5)	9.7425(4)	20.831(16)	12.166(4)
b (Å)	10.104(5)	9.7964(4)	9.137(6)	17.6501(10)
c (Å)	10.837(6)	10.3959(5)	20.062(15)	14.104(7)
α (°)	67.98(2)	77.9630(10)	90	90
β (°)	76.875(19)	81.9760(10)	96.34(3)	114.646(11)
γ (°)	67.945(15)	69.6560(10)	90	90
V(Å^3)	868.7(8)	907.42(7)	3795(5)	2752.7(17)
Z	2	1	8	4
D_{calcd} (Mg/m^3)	1.701	1.807	1.527	1.543
μ(mm^{-1})	1.294	1.239	0.730	0.541
Temperature (K)	293(2)	296(2)	293(2)	295(2)
F(000)	452	489	1776	1308
R_{int}	0.0384	0.0253	0.0828	0.0581
R_1 [$I > 2\sigma(I)$][a]	0.0344	0.0236	0.0518	0.0658
wR_2 [$I > 2\sigma(I)$][b]	0.0829	0.0606	0.1044	0.1619
Gof	1.065	1.047	1.035	1.044

[a] $R_1 = \Sigma||F_o|-|F_c||/\Sigma|F_o|$, [b] $wR_2 = [\Sigma w(F_o^2-F_c^2)^2]/\Sigma w(F_o^2)^2]^{1/2}$

Table S2 Selected bond lengths (Å) and angles (º) for **1 – 4**.

CP **1**							
Cu(1)-O(3)	1.9254(17)	Cu(1)-O(2)$^{\#2}$	2.264(2)	Cu(1)-N(1)	2.045(2)	Cu(1)-N(2)	2.025(2)
Cu(1)-O(1)$^{\#1}$	1.9269(17)	O(3)-Cu(1)-O(1)$^{\#1}$	98.41(8)	O(3)-Cu(1)-N(2)	88.35(8)	O(1)$^{\#1}$-Cu(1)-N(2)	166.61(8)
O(3)-Cu(1)-N(1)	166.50(7)	N(2)-Cu(1)-N(1)	80.78(8)	O(1)$^{\#1}$-Cu(1)-O(2)$^{\#2}$	99.08(8)	N(1)-Cu(1)-O(2)$^{\#2}$	83.15(8)
O(1)$^{\#1}$-Cu(1)-N(1)	90.73(8)	O(3)-Cu(1)-O(2)$^{\#2}$	105.01(8)	N(2)-Cu(1)-O(2)$^{\#2}$	90.22(8)		
Symmetry codes: #1 -*x*+1, -*y*+1, -*z*+1; #2 -*x*+1, -*y*, -*z*+1.							
CP **2**							
Cd(1)-O(1)	2.2820(19)	Cd(1)-O(2)$^{\#2}$	2.3457(18)	Cd(1)-O(3)$^{\#1}$	2.4515(17)	Cd(1)-N(1)	2.376(2)
Cd(1)-O(4)$^{\#1}$	2.3006(17)	Cd(1)-N(2)	2.3571(19)	O(1)-Cd(1)-O(4)$^{\#1}$	116.18(8)	O(1)-Cd(1)-O(2)$^{\#2}$	122.48(7)
O(1)-Cd(1)-N(2)	82.54(7)	O(4)$^{\#1}$-Cd(1)-O(2)$^{\#2}$	85.97(7)	N(2)-Cd(1)-N(1)	70.39(7)	O(2)$^{\#2}$-Cd(1)-O(3)$^{\#1}$	139.33(6)
O(4)$^{\#1}$-Cd(1)-N(2)	160.71(8)	O(4)$^{\#1}$-Cd(1)-N(1)	97.98(8)	O(1)-Cd(1)-O(3)$^{\#1}$	87.48(7)	N(2)-Cd(1)-O(3)$^{\#1}$	135.90(6)
O(2)$^{\#2}$-Cd(1)-N(2)	79.42(7)	O(2)$^{\#2}$-Cd(1)-N(1)	92.54(7)	O(4)$^{\#1}$-Cd(1)-O(3)$^{\#1}$	54.48(6)	N(1)-Cd(1)-O(3)$^{\#1}$	84.90(7)
O(1)-Cd(1)-N(1)	130.83(7)						
Symmetry codes: #1 -x+1, -y, -z+1; #2 -x+1, -y+1, -z+1.							
CP **3**							
Mn(1)-O(2)	2.096(2)	Mn(1)-O(4)$^{\#2}$	2.184(3)	Mn(1)-O(3)$^{\#2}$	2.332(2)	Mn(1)-N(2)	2.286(3)
Mn(1)-O(1)$^{\#1}$	2.113(2)	Mn(1)-N(1)	2.275(3)	O(2)-Mn(1)-O(1)$^{\#1}$	93.86(8)	O(2)-Mn(1)-O(4)$^{\#2}$	101.05(9)
O(2)-Mn(1)-N(1)	98.13(10)	O(1)$^{\#1}$-Mn(1)-O(4)$^{\#2}$	99.61(9)	N(1)-Mn(1)-N(2)	72.38(10)	O(4)$^{\#2}$-Mn(1)-O(3)$^{\#2}$	57.99(9)
O(1)$^{\#1}$-Mn(1)-N(1)	97.07(10)	O(1)$^{\#1}$-Mn(1)-N(2)	164.88(10)	O(2)-Mn(1)-O(3)$^{\#2}$	158.30(8)	N(1)-Mn(1)-O(3)$^{\#2}$	103.51(10)
O(4)$^{\#2}$-Mn(1)-N(1)	153.55(9)	O(4)$^{\#2}$-Mn(1)-N(2)	86.91(9)	O(1)$^{\#1}$-Mn(1)-O(3)$^{\#2}$	85.12(9)	N(2)-Mn(1)-O(3)$^{\#2}$	86.87(9)
O(2)-Mn(1)-N(2)	98.29(9)						
Symmetry codes: #1 -*x*+1/2, -*y*+3/2, -*z*+1; #2 -*x*+1/2, *y*+1/2, -*z*+1/2.							
CP **4**							
Mn(1)-O(3)	2.114(3)	Mn(1)-N(1)	2.280(11)	Mn(1)-O(2)$^{\#2}$	2.268(3)	Mn(1)-N(2)	2.258(12)
O(3)$^{\#1}$-Mn(1)-N(1)	90.7(6)	O(3)-Mn(1)-O(3)$^{\#1}$	167.62(14)	O(3)-Mn(1)-O(2)$^{\#2}$	89.63(11)	N(2)-Mn(1)-O(2)$^{\#3}$	83.9(5)
N(2)-Mn(1)-N(1)	73.2(2)	O(3)-Mn(1)-N(2)	88.7(6)	N(2)-Mn(1)-O(2)$^{\#2}$	158.2(5)	O(2)$^{\#2}$-Mn(1)-O(2)$^{\#3}$	117.49(15)
O(2)$^{\#2}$-Mn(1)-N(1)	85.6(5)	O(3)$^{\#1}$-Mn(1)-N(2)	101.2(6)	O(3)-Mn(1)-O(2)$^{\#3}$	83.95(11)	O(3)-Mn(1)-N(1)	99.4(6)
O(2)$^{\#3}$-Mn(1)-N(1)	156.8(5)						
Symmetry codes: #1 -*x*+1/2, *y*, -*z*+1; #2 *x*-1, *y*, *z*; #3 -*x*+3/2, *y*, -*z*+1.							